Search for Extraterrestrial Point Sources of Neutrinos with AMANDA-II

J. Ahrens,[11] X. Bai,[1] S.W. Barwick,[10] T. Becka,[11] J. K. Becker,[2] E. Bernardini,[4] D. Bertrand,[3] F. Binon,[3] A. Biron,[4] D. J. Boersma,[4] S. Böser,[4] O. Botner,[17] A. Bouchta,[17] O. Bouhali,[3] T. Burgess,[18] S. Carius,[6] T. Castermans,[13] A. Chen,[15] D. Chirkin,[9] B. Collin,[8] J. Conrad,[17] J. Cooley,[15] D. F. Cowen,[8] A. Davour,[17] C. De Clercq,[19] T. DeYoung,[12] P. Desiati,[15] J. P. Dewulf,[3] P. Ekström,[18] T. Feser,[11] T. K. Gaisser,[1] R. Ganugapati,[15] M. Gaug,[4] H. Geenen,[2] L. Gerhardt,[10] A. Goldschmidt,[7] A. Groß,[2] A. Hallgren,[17] F. Halzen,[15] K. Hanson,[15] R. Hardtke,[15] T. Harenberg,[2] T. Hauschildt,[4] K. Helbing,[7] M. Hellwig,[11] P. Herquet,[13] G. C. Hill,[15] D. Hubert,[19] B. Hughey,[15] P. O. Hulth,[18] K. Hultqvist,[18] S. Hundertmark,[18] J. Jacobsen,[7] A. Karle,[15] M. Kestel,[8] L. Köpke,[11] M. Kowalski,[4] K. Kuehn,[10] J. I. Lamoureux,[7] H. Leich,[4] M. Leuthold,[4] P. Lindahl,[6] I. Liubarsky,[5] J. Madsen,[16] K. Mandli,[15] P. Marciniewski,[17] H. S. Matis,[7] C. P. McParland,[7] T. Messarius,[2] Y. Minaeva,[18] P. Miočinović,[9] R. Morse,[15] K. Münich,[2] R. Nahnhauer,[4] T. Neunhöffer,[11] P. Niessen,[19] D. R. Nygren,[7] H. Ögelman,[15] Ph. Olbrechts,[19] C. Pérez de los Heros,[17] A. C. Pohl,[6] R. Porrata,[9] P. B. Price,[9] G. T. Przybylski,[7] K. Rawlins,[15] E. Resconi,[4] W. Rhode,[2] M. Ribordy,[13] S. Richter,[15] J. Rodríguez Martino,[18] H. G. Sander,[11] K. Schinarakis,[2] S. Schlenstedt,[4] T. Schmidt,[4] D. Schneider,[15] R. Schwarz,[15] A. Silvestri,[10] M. Solarz,[9] G. M. Spiczak,[16] C. Spiering,[4] M. Stamatikos,[15] D. Steele,[15] P. Steffen,[4] R. G. Stokstad,[7] K. H. Sulanke,[4] I. Taboada,[14] L. Thollander,[18] S. Tilav,[1] W. Wagner,[2] C. Walck,[18] Y. R. Wang,[15] C. H. Wiebusch,[2] C. Wiedemann,[18] R. Wischnewski,[4] H. Wissing,[4] K. Woschnagg,[9] and G. Yodh[10]

[1]*Bartol Research Institute, University of Delaware, Newark, Delaware 19716, USA*
[2]*Fachbereich 8 Physik, BU Wuppertal, D-42097 Wuppertal, Germany*
[3]*Université Libre de Bruxelles, Science Faculty CP230, Boulevard du Triomphe, B-1050 Brussels, Belgium*
[4]*DESY-Zeuthen, D-15735, Zeuthen, Germany*
[5]*Blackett Laboratory, Imperial College, London SW7 2BW, United Kingdom*
[6]*Department of Technology, Kalmar University, S-39182 Kalmar, Sweden*
[7]*Lawrence Berkeley National Laboratory, Berkeley, California 94720, USA*
[8]*Department of Physics, Pennsylvania State University, University Park, Pennsylvania 16802, USA*
[9]*Department of Physics, University of California, Berkeley, California 94720, USA*
[10]*Department of Physics and Astronomy, University of California, Irvine, California 92697, USA*
[11]*Institute of Physics, University of Mainz, Staudinger Weg 7, D-55099 Mainz, Germany*
[12]*Department of Physics, University of Maryland, College Park, Maryland 20742, USA*
[13]*University of Mons-Hainaut, 7000 Mons, Belgium*
[14]*Departamento de Física, Universidad Simón Bolívar, Caracas 1080, Venezuela*
[15]*Department of Physics, University of Wisconsin, Madison, Wisconsin 53706, USA*
[16]*Physics Department, University of Wisconsin, River Falls, Wisconsin 54022, USA*
[17]*Division of High Energy Physics, Uppsala University, S-75121 Uppsala, Sweden*
[18]*Department of Physics, Stockholm University, SE-10691 Stockholm, Sweden*
[19]*Vrije Universiteit Brussel, Dienst ELEM, B-1050 Brussels, Belgium*

(Received 19 September 2003; published 19 February 2004)

We present the results of a search for point sources of high-energy neutrinos in the northern hemisphere using AMANDA-II data collected in the year 2000. Included are flux limits on several active-galactic-nuclei blazars, microquasars, magnetars, and other candidate neutrino sources. A search for excesses above a random background of cosmic-ray-induced atmospheric neutrinos and misreconstructed downgoing cosmic-ray muons reveals no statistically significant neutrino point sources. We show that AMANDA-II has achieved the sensitivity required to probe known TeV γ-ray sources such as the blazar Markarian 501 in its 1997 flaring state at a level where neutrino and γ-ray fluxes are equal.

DOI: 10.1103/PhysRevLett.92.071102 PACS numbers: 95.85.Ry, 96.40.Tv

Introduction.—The search for sources of high-energy extraterrestrial neutrinos is the primary mission of the Antarctic Muon and Neutrino Detector Array (AMANDA). The mechanism for accelerating cosmic rays to energies above the "knee" (10^{15} eV) remains a mystery. Cosmic rays are thought to be accelerated in the shock fronts of galactic objects such as supernova remnants, microquasars, and magnetars, and in extragalactic sources such as the cores of active galactic nuclei and gamma ray bursts [1].

High energy protons accelerated in these objects will collide with the ambient gas and radiation surrounding the acceleration region, or with matter or radiation intervening between the source and the earth. This leads to pion production, the charged pions decaying into highly energetic muon and electron neutrinos, and the neutral

pions decaying into the observed γ rays. Fermi acceleration of charged particles in magnetic shocks naturally leads to power-law spectra, E^{α}, where α is typically close to -2. By the time the neutrinos reach the earth, vacuum oscillations will have uniformly populated all three flavors (unless the neutrinos are unstable [2]). All limits quoted in this Letter are on the muon neutrino flux arriving at the earth; limits at the source will be approximately a factor of 2 higher due to oscillations.

Neutrino astronomy may provide information complementary to the knowledge obtained from high-energy photons and charged particles. Accelerated electrons and protons can both result in the production of high-energy gamma rays, so only neutrinos can distinguish between electromagnetic and hadronic processes. Since neutrinos propagate directly from their point of origin undeflected by magnetic fields, they have the potential to reveal ''hidden'' sources masked by photon absorption. Probing the neutrino sky may bring us closer to solving the cosmic-ray mystery, or might even reveal something completely new and unexpected.

The AMANDA-II detector.—AMANDA-II [3] is a Cherenkov detector frozen into the antarctic polar ice cap. A high-energy muon neutrino interacting with the ice or bedrock in the vicinity of the detector results in a high-energy muon propagating up to tens of kilometers.

The muon track is reconstructed based on detection of the Cherenkov light emitted as it propagates through a 19-string array of 677 photomultiplier tubes. The median neutrino pointing resolution is 2°–2.5°, depending weakly on declination, and is dominated by the resolution of the muon track reconstruction. AMANDA-II demonstrates a significant improvement over its predecessor in acceptance and background rejection, especially near the horizon. Results from the first phase of AMANDA, the ten-string subdetector AMANDA-B10, have been reported in [4].

Atmospheric muons from cosmic rays that penetrate to AMANDA depths are the dominant background. AMANDA-II views the neutrino sky above the northern hemisphere using the earth as an atmospheric muon filter. Cosmic rays also produce neutrinos in the earth's atmosphere, but with a spectral index of $\alpha = -3.7$, softer than expected for astrophysical sources. Atmospheric neutrinos are an important source for calibration in AMANDA [5], but are also background to a search for extraterrestrial point sources. A point source search is conducted by looking for excess events above the background, which is experimentally measured for a given angular search bin by taking the average background rate in the same band of declination.

Data processing and detector simulation.— The data set comprises 1.2×10^9 triggered events collected over 238 days between February and November, 2000, with 197.0 days live time after correcting for 17.2% detector dead time. After application of an iterative series of maximum-likelihood reconstruction algorithms, 2.1 million events reconstructed with declination $\delta > 0°$ remain in the experimental sample.

To prevent bias in the selection of cuts, the data are ''blinded'' by randomizing the reconstructed right ascension (RA) angle of each event. The output of a neural network (NN) trained on simulated events and using six input variables (such as the number of unscattered photon hits, track length, likelihood of the muon track reconstruction, and topological variables [5]) is used as a quality cut. A second cut is placed on the likelihood ratio (LR) between the muon track reconstruction and a muon reconstruction weighted by an atmospheric muon prior [6]. The prior describes the zenith-dependent frequency of downgoing muons such that choosing a cut on the LR gives downgoing hypotheses a prior weight of up to 10^6 more than the upgoing hypotheses, effectively forcing events surviving the cut to be of higher quality. The final choice of NN quality cut, likelihood ratio cut, and the optimum size for a search bin are determined independently in each 5° band of declination (Dec.) in order to optimize the limit setting potential of the experiment [7]. The directional information is then restored (data ''unblinded'') for the calculation of the limits and significances.

A full simulation chain [4] including neutrino absorption in the earth, neutral current regeneration, muon propagation, and detector response is used to simulate the point source signal according to an E^{-2} energy spectrum. The limits obtained in this analysis are a function of the measured background, n_b, as well as the expected number of events, n_s, from a simulated flux $\Phi(E)$: $\Phi_{\text{limit}}(E) = \Phi(E) \times \mu_{90}(n_{\text{obs}}, n_b)/n_s$, where n_{obs} is the number of observed events in the given source bin, and μ_{90} is the 90% upper limit on the number of events following the unified ordering prescription of Feldman and Cousins [8].

Systematic uncertainties.—Atmospheric neutrinos were used to determine the absolute normalization of the detector simulation. The normalization factor 0.86 is consistent with the theoretical uncertainty of 25% on the atmospheric neutrino flux [5,9]. The overall systematic uncertainty, which includes the theoretical uncertainty of the atmospheric neutrino flux and statistical uncertainty of the measured background, is incorporated into the limits using the Cousins-Highland [10] prescription with unified Feldman-Cousins ordering [8,11] but with a more appropriate choice of the likelihood ratio test [12].

Coincident events between the SPASE air shower array [13] and AMANDA-II were used to evaluate the systematic error in pointing accuracy. This value was determined to be less than 1°, which results in signal loss in a typical search bin of only 5%.

Results.—The final sample consists of 699 upwardly reconstructed ($\delta > 0°$) events, illustrated in Fig. 1. A comparison to the normalized atmospheric neutrino

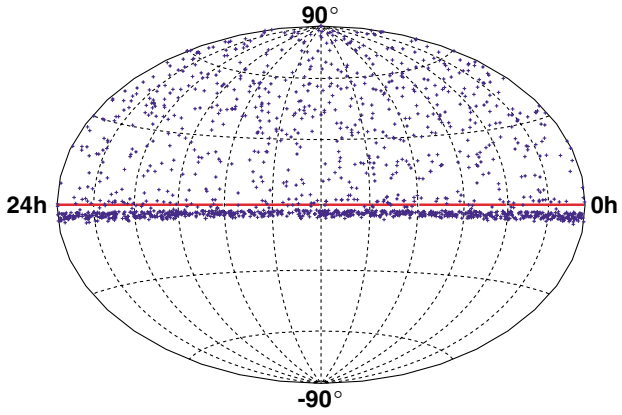

FIG. 1 (color online). Final point source search sample plotted in equatorial coordinates. The thick band of events at $\delta < 0$ shows the onset of cosmic muon background contamination.

simulation reveals that for declinations $\delta > 5°$ the sample is strongly dominated by atmospheric neutrinos.

A binned search for excesses in the region $0° < \delta < 85°$ has been performed. The search grid contains 301 rectangular bins with zenith-dependent widths ranging from 6° to 10°, based on the aforementioned bin-size optimization. The grid is shifted 4 times in declination and right ascension to fully cover boundaries between the bins of the original configuration. The number of times to shift the grid was studied, taking into account statistical penalties for the number of shifts by using simulated event samples, and set at a level where further shifts do not markedly improve the average maximum significance obtained on simulated Poisson-fluctuated signals of similar magnitude to the background.

The most significant excess, observed at about 68° Dec., 21.1 h RA, is eight events observed on an expected background of 2.1. Simulation reveals a probability of 51% to observe such an excess as a random upward fluctuation of the background.

In addition to the binned search, we place limits on a number of extragalactic and galactic candidate sources. Circular bins with optimized radii are positioned at each candidate position; the number of expected background events is given by the number of observed events in the declination band scaled down to the search bin area. The same method applied to any point in the northern hemisphere yields neutrino flux upper limits shown in Fig. 2. For the region $\delta > 85°$, an adjacent region at lower declination was used for the background estimation. The average flux upper limits for E^{-2} spectra obtained in an ensemble of identical experiments in the case of no true signal is shown vs declination in Fig. 3. It should be pointed out that due to the large number of cells tested a single source with a flux at the sensitivity level (90% average flux upper limit) would normally be interpreted as a statistical fluctuation. Therefore a flux a few times higher would be needed to make a discovery of a point source possible in the binned search.

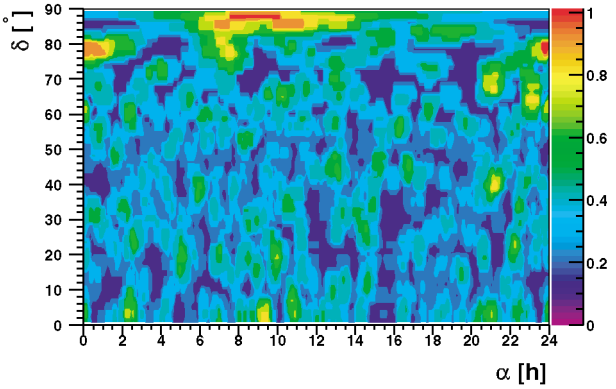

FIG. 2 (color). Neutrino flux upper limits (90% confidence level) in equatorial coordinates. Limits (scale on right axis) are in units of 10^{-7} cm^{-2} s^{-1} for an assumed E^{-2} spectrum, integrated above $E_\nu = 10$ GeV. Systematic uncertainties are not included.

In Table I, we present neutrino flux limits for northern hemisphere TeV blazars, selected GeV blazars, microquasars, magnetars, and selected miscellaneous candidates. The limits are computed based on an assumed E^{-2} energy spectrum. Limits for other spectra can be computed using the neutrino effective area shown in Fig. 4: The neutrino flux limit for an assumed flux $d\Phi/dE \propto E^\alpha$ is inversely proportional to the energy averaged effective area $\overline{A}_{\rm eff}(\alpha) = \int_{E_{\rm min}}^{\infty} A_{\rm eff}(E) E^\alpha \, dE / \int_{E_{\rm min}}^{\infty} E^\alpha \, dE$. Effective areas at declinations not shown in Fig. 4 can be obtained by linear interpolation in δ; the systematic shift induced by this interpolation is below 20% for spectral indices in the range $\alpha = -1.5$ to -2.5. Integrated neutrino flux limits are strongly dependent on the spectral index, while the differential sensitivities $d\Phi/dE$ remain approximately constant at the energy at which most events are detected. This energy ranges from about 30 TeV at

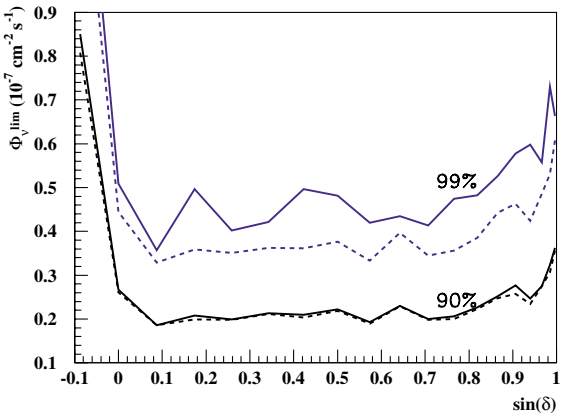

FIG. 3 (color online). Average flux upper limits (90% and 99% confidence) for an E^{-2} signal hypothesis, integrated above $E_\nu = 10$ GeV, are shown vs declination (δ), solid lines with and dashed lines without the inclusion of systematic uncertainty (as described in the text). The limits worsen near the horizon due to the onset of cosmic ray muon contamination.

TABLE I. 90% upper limits on candidate sources. The number of events observed within the search bin is denoted by n_{obs}, and n_b is the number of expected background events determined by measuring the background off-source in the same declination band. Limits are for an assumed E_ν^{-2} spectral shape, integrated above $E_\nu = 10$ GeV, and presented in units of 10^{-15} cm^{-2} s^{-1}(Φ_μ) and 10^{-8} cm^{-2} s^{-1}(Φ_ν).

Candidate	Dec. [°]	RA [h]	n_{obs}	n_b	Φ_μ^{lim}	Φ_ν^{lim}
TeV Blazars						
Markarian 421	38.2	11.07	3	1.50	3.0	3.5
Markarian 501	39.8	16.90	1	1.57	1.5	1.8
1ES 1426 + 428	42.7	14.48	1	1.62	1.4	1.7
1ES 2344 + 514	51.7	23.78	1	1.23	1.6	2.0
1ES 1959 + 650	65.1	20.00	0	0.93	0.9	1.3
GeV Blazars						
QSO 0528 + 134	13.4	5.52	1	1.09	2.5	2.0
QSO 0235 + 164	16.6	2.62	1	1.49	2.0	1.7
QSO 1611 + 343	34.4	16.24	0	1.29	0.7	0.8
QSO 1633 + 382	38.2	16.59	1	1.50	1.5	1.7
QSO 0219 + 428	42.9	2.38	1	1.63	1.4	1.6
QSO 0954 + 556	55.0	9.87	1	1.66	1.3	1.7
QSO 0716 + 714	71.3	7.36	2	0.74	2.9	4.4
Microquasars						
SS433	5.0	19.20	0	2.38	1.0	0.7
GRS 1915 + 105	10.9	19.25	1	0.91	2.9	2.2
GRO J0422 + 32	32.9	4.36	2	1.31	2.9	2.9
Cygnus X1	35.2	19.97	2	1.34	2.2	2.5
Cygnus X3	41.0	20.54	3	1.69	3.0	3.5
XTE J1118 + 480	48.0	11.30	1	0.92	1.7	2.2
CI Cam	56.0	4.33	0	1.72	0.6	0.8
LS I +61 303	61.2	2.68	0	0.75	1.0	1.5
SNR, magnetars, and miscellaneous						
SGR 1900 + 14	9.3	19.12	0	0.97	1.4	1.0
Crab Nebula	22.0	5.58	2	1.76	2.6	2.4
Cassiopeia A	58.8	23.39	0	1.01	0.9	1.2
3EG J0450 + 1105	11.4	4.82	2	0.89	4.2	3.2
M 87	12.4	12.51	0	0.95	1.3	1.0
Geminga	17.9	6.57	3	1.78	3.7	3.3
UHE CR Triplet	20.4	1.28	2	1.84	2.4	2.3
NGC 1275	41.5	3.33	1	1.72	1.4	1.6
Cygnus OB2 region [14]	41.5	20.54	3	1.72	2.9	3.5
UHE CR Triplet	56.9	12.32	1	1.48	1.4	1.9

$\delta = 0 - 30°$ to 10 TeV at $\delta > 30°$, and the changes at these energies are below 30% for $\alpha = -2$ to -2.75. The integrated muon flux limits for a softer spectrum $\alpha = -2.75$ are worse by a factor ~ 5 ($\delta > 45°$) to 10 ($\delta \approx 0°$–$15°$) compared to $\alpha = -2$.

In [15], expected numbers of neutrino induced muon events for galactic microquasars using source parameters estimated from radio observations are calculated. For microquasars whose jets have not been resolved in the radio band, the neutrino emission is estimated from the synchrotron luminosity. In the case of the microquasar SS433, 252 muons yr^{-1} km^{-2} are predicted. Scaling to the AMANDA-II effective area at that declination ($A_{\text{eff}}^{\mu} = 7900$ m^2) and to the live time of this analysis yields a prediction of 1.07 events for an assumed E^{-2} spectrum. We observe no events in the search bin for this source, and place a 90% upper limit of 1.24 events. Because of a random fluctuation, this limit is about 3 times better than the sensitivity at this declination.

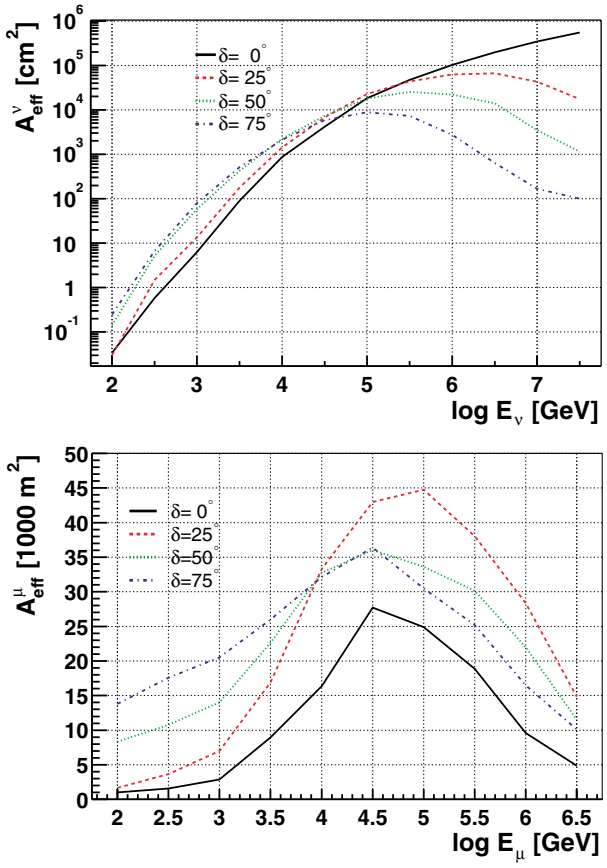

FIG. 4 (color online). Neutrino and muon effective areas vs energy at different declinations (δ). E_μ is the muon energy at the closest approach to the center of the detector. The effect of neutrino absorption in the earth is included in the neutrino effective areas.

In Fig. 5, the AMANDA-II neutrino sensitivity is compared to the 1997-averaged TeV γ-ray flux of the blazar Markarian 501 ($z = 0.031$), and the intrinsic source spectrum (corrected for IR absorption). The figure demonstrates AMANDA-II has achieved the sensitivity needed to search for neutrino fluxes from TeV γ-ray sources of similar strength to the intrinsic γ-ray flux.

Conclusions.—One year of AMANDA-II data has been searched for clusters of neutrino events. No significant excesses have been found, and flux limits for 30 candidate sources have been calculated. For some candidates, the limits are close to neutrino flux predictions. Data collected in 2001–2002 are being analyzed and should improve the sensitivity of this analysis approximately by a factor 2.3.

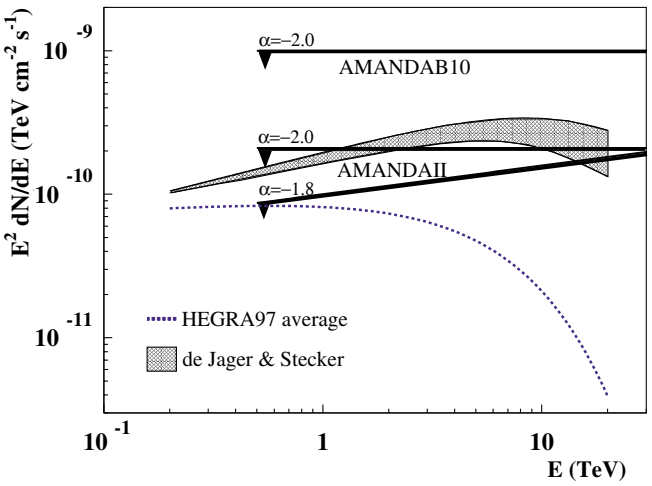

FIG. 5 (color online). The AMANDA-II 90% average flux upper limit (197 days live time) for two assumed spectral indices (α) is compared to the average γ-ray flux of Markarian 501 as observed in 1997 by the HEGRA system of air Cherenkov telescopes [16]. These average upper limits are based on the assumption that the neutrino spectrum extends to beyond 10 PeV. Also shown is the intrinsic source flux after correction for IR absorption by de Jager and Stecker [17]. The shaded area is bounded by two curves corresponding to different models of galactic luminosity evolution. For comparison, the AMANDA-B10 result [4] is also shown.

We acknowledge the support of the following agencies: National Science Foundation–Office of Polar Programs, National Science Foundation–Physics Division, University of Wisconsin Alumni Research Foundation, Department of Energy, and National Energy Research Scientific Computing Center (supported by the Office of Energy Research of the Department of Energy), UC-Irvine AENEAS Supercomputer Facility, U.S.A.; Swedish Research Council, Swedish Polar Research Secretariat, and Knut and Alice Wallenberg Foundation, Sweden; German Ministry for Education and Research, Deutsche Forschungsgemeinschaft (DFG), Germany; Fund for Scientific Research (FNRS-FWO), Flanders Institute to encourage scientific and technological research in industry (IWT), and Belgian Federal Office for Scientific, Technical and Cultural affairs (OSTC), Belgium; Fundación Venezolana de Promoción al Investigador (FVPI), Venezuela; D. F. C. acknowledges the support of the NSF CAREER program.

[1] F. Halzen and D. Hooper, Rep. Prog. Phys. **65**, 1025 (2002).
[2] J. F. Beacom *et al.*, Phys. Rev. D **68**, 093005 (2003).
[3] E. Andrés *et al.*, Nature (London) **410**, 441 (2001).
[4] J. Ahrens *et al.*, Astrophys. J. **583**, 1040 (2003).
[5] J. Ahrens *et al.*, Phys. Rev. D **66**, 012005 (2002).
[6] G. C. Hill, in *Proceedings of the 27th ICRC*, edited by G. Heinzelmann *et al.* (Copernicus Gesellschaft, Hamburg, Germany, 2001), p. 1279.
[7] G. C. Hill and K. Rawlins, Astropart. Phys. **19**, 393 (2003).
[8] G. J. Feldman and R. D. Cousins, Phys. Rev. D **57**, 3873 (1998).
[9] P. Lipari, Astropart. Phys. **1**, 195 (1993).
[10] R. D. Cousins and V. L. Highland, Nucl. Instrum. Methods Phys. Res., Sect. A **320**, 331 (1992).
[11] J. Conrad *et al.*, Phys. Rev. D **67**, 012002 (2003).
[12] G. C. Hill, Phys. Rev. D **67**, 118101 (2003).
[13] J. Ahrens *et al.*, Nucl. Instrum. Methods Phys. Res., Sect. A (to be published)
[14] An unidentified TeV γ-ray source; see F. Aharonian *et al.*, Astron. Astrophys. **393**, L37 (2002).
[15] C. Distefano, D. Guetta, A. Levinson, and E. Waxmann, Astrophys. J. **575**, 378 (2002).
[16] F. Aharonian *et al.*, Astron. Astrophys. **393**, 89 (2002).
[17] O. C. de Jager and F. W. Stecker, Astrophys. J. **566**, 738 (2002).